Eur. Phys. J. B **22**, 213–221 (2001)

THE EUROPEAN PHYSICAL JOURNAL B

EDP Sciences
© Società Italiana di Fisica
Springer-Verlag 2001

Spike autosolitons and pattern formation scenarios in the two-dimensional Gray-Scott model

C.B. Muratov[1,a] and V.V. Osipov[2]

[1] Department of Mathematical Sciences and Center for Applied Mathematics and Statistics, New Jersey Institute of Technology, University Heights, Newark, NJ 07102, USA
[2] CSIC, Laboratorio de Fisica de Sistemas Pequeños y Nanotecnologia, Calle Serrano, 144, 28006, Madrid, Spain

Received 6 November 2000 and Received in final form 27 February 2001

Abstract. We performed an extensive numerical study of pattern formation scenarios in the two-dimensional Gray-Scott reaction-diffusion model. We concentrated on the parameter region in which there exists a strong separation of length and/or time scales. We found that the static one-dimensional autosolitons (stripes) break up into two-dimensional radially-symmetric autosolitons (spots). The traveling one-dimensional autosolitons (wave fronts) can be stable or undergo breakup. The static two-dimensional radially-symmetric autosolitons may break up and self-replicate leading to the formation of space-filling patterns of spots, wave fronts, or spatio-temporal chaos due to the competition of self-replication and annihilation of spots upon collision.

PACS. 47.54.+r Pattern selection; pattern formation – 82.20.-w Chemical kinetics and dynamics – 05.45.-a Nonlinear dynamics and nonlinear dynamical systems

1 Introduction

Self-organization and pattern formation in nonequilibrium systems are among the most fascinating phenomena in nonlinear physics [1–11]. Pattern formation is observed in various physical systems including fluids, gas and electron-hole plasmas, various semiconductor, superconductor and gas-discharge structures, some ferroelectric, magnetic and optical media; combustion systems (see, for example, [5,9–14]), as well as many chemical and biological systems (see, for example, [1–7,15]).

Self-organization is often associated with the destabilization of the uniform state of the system [1–5, 10, 11]. At the same time, when the uniform state of the system is stable, one can excite large-amplitude patterns, including *autosolitons* (ASs) — self-sustained solitary inhomogeneous states, by applying a sufficiently strong stimulus [8–11, 16–19]. Autosolitons are elementary objects in open dissipative systems away from equilibrium. They share the properties of both solitons and traveling waves (or autowaves, as they are also referred to [2,6]). They are similar to solitons since they are localized objects whose existence is due to the nonlinearities of the system. On the other hand, from the physical point of view they are essentially different from solitons in the fact that they are *dissipative structures*, that is, they are self-sustained objects which form in strongly dissipative systems as a result of the balance between the dissipation and pumping of energy or matter. This is the reason why, in contrast to solitons, their properties are independent of the initial conditions and are determined primarily by the nonlinearities of the system [8–11]. ASs can be static, pulsating, or traveling. As a result of their various instabilities, these simplest localized patterns can spontaneously transform into complex space-filling static or dynamic patterns, including complex pulsating and traveling patterns, or spatio-temporal chaos [8–14, 18–33]. Thus, it is the destabilization of the ASs that is the main source of self-organization in nonequilibrium systems with the stable homogeneous state.

A classical example of a system of this kind is the Gray-Scott model of an autocatalytic chemical reaction [34]. Recently, we showed that this model is capable of supporting various kinds of ASs [35–37] (see also [38–40]). A characteristic feature of these autosolitons is that they have the shape of narrow spikes in the distribution of the activator substance. Under certain conditions, they undergo instabilities that should lead to the formation of more complex patterns [35, 38, 41].

In this paper, we perform a numerical study of the spike patterns in the Gray-Scott model in two dimensions. We will study the parameter region in which there exists a strong separation between the length and/or time scales of the activator and the inhibitor. We will study the initial formation of the spike ASs and investigate their transformations into more complex patterns. The outline of our paper is as follows. In Section 2 we introduce the model

[a] e-mail: muratov@m.njit.edu

we will study, in Section 3 we present the results of our numerical simulations, and in Section 4 we give the summary of our work and draw conclusions.

2 The model

The Gray-Scott model describes the kinetics of a simple autocatalytic reaction in an unstirred flow reactor. The reactor is a narrow space between two porous walls. Substance Y whose concentration is kept fixed outside of the reactor is supplied through the walls into the reactor with the rate k_0 and the products of the reaction are removed from the reactor with the same rate. Inside the reactor Y undergoes the reaction involving an intermediate species X:

$$2X + Y \xrightarrow{k_1} 3X, \tag{1}$$

$$X \xrightarrow{k_2} \text{inert}. \tag{2}$$

The first reaction is a cubic autocatalytic reaction resulting in self-production of species X; therefore, X is the activator species. On the other hand, the production of X is controlled by species Y, so Y is the inhibitor species. The equations of chemical kinetics which describe the spatiotemporal variations of the concentrations of X and Y in the reactor and take into account the supply and the removal of the substances through the porous walls take the following form [34]:

$$\frac{\partial X}{\partial t} = -(k_0 + k_2)X + k_1 X^2 Y + D_X \Delta X, \tag{3}$$

$$\frac{\partial Y}{\partial t} = k_0(Y_0 - Y) - k_1 X^2 Y + D_Y \Delta Y, \tag{4}$$

where now X and Y are the concentrations of the activator and the inhibitor species, respectively, Y_0 is the concentration of Y in the reservoir, Δ is the two-dimensional Laplacian, and D_X and D_Y are the diffusion coefficients of X and Y.

In order to be able to understand various pattern formation phenomena in a system of this kind, it is crucial to introduce the variables and the time and length scales that truly represent the physical processes acting in the system. The first and the most important is the choice of the characteristic time scales. These are primarily dictated by the time constants of the dissipation processes. For Y this is the supply and the removal with the rate k_0, whereas for X this is the removal from the system and the decay via the second reaction with the total rate $k_0 + k_2$. A natural way to introduce the dimensionless inhibitor concentration is to scale it with Y_0. Since we want to fix the time scale of the variation of the inhibitor (with the fixed activator), we will rescale X in such a way that the reaction term in equation (4) will generate the same time scale as the dissipative term. This leads to the following dimensionless quantities:

$$\theta = X/X_0, \quad \eta = Y/Y_0, \quad X_0 = \left(\frac{k_0}{k_1}\right)^{1/2}. \tag{5}$$

The characteristic time and length scales for these quantities are

$$\tau_\theta = (k_0 + k_2)^{-1}, \quad \tau_\eta = k_0^{-1}, \tag{6}$$

$$l = (D_X \tau_\theta)^{1/2}, \quad L = (D_Y \tau_\eta)^{1/2}. \tag{7}$$

Naturally, one should require positivity of θ and η.

Let us introduce the dimensionless parameters $\epsilon = l/L$, $\alpha = \tau_\theta/\tau_\eta$, and A:

$$\epsilon = \sqrt{\frac{D_X k_0}{(k_0 + k_2) D_Y}}, \tag{8}$$

$$\alpha = \frac{k_0}{k_0 + k_2} \tag{9}$$

$$A = \frac{Y_0 k_0^{1/2} k_1^{1/2}}{(k_0 + k_2)}. \tag{10}$$

The parameter A is the dimensionless strength of the activation process, that is, it describes the degree of deviation of the system from thermal equilibrium. Then, equations (3) and (4) can be rewritten in the following dimensionless form

$$\alpha \frac{\partial \theta}{\partial t} = \epsilon^2 \Delta\theta + A\theta^2\eta - \theta, \tag{11}$$

$$\frac{\partial \eta}{\partial t} = \Delta\eta - \theta^2\eta + 1 - \eta, \tag{12}$$

provided that length and time are measured in the units of L and τ_η, respectively. We will assume that the problem is defined on the sufficiently large finite domain with zero flux boundary conditions. Notice that the kinetic model used to arrive at equations (11) and (12) imposes a restriction $\alpha \leq 1$ (see Eq. (6)). For the sake of generality, in the following we will allow α to take arbitrary values.

According to the general qualitative theory of ASs [11], the types of the ASs realized in a system of this kind are mainly determined by the values of ϵ and α and the shape of the nullclines of equations (11) and (12). These nullclines are shown in Figure 1. From this figure one can see that the nullcline of the equation for the activator is Λ-shaped [11]. This means that spike patterns can be realized in this system [11].

One can easily check that for $0 < A < 2$ there is only one stationary homogeneous state $\theta = \theta_\mathrm{h}$ and $\eta = \eta_\mathrm{h}$:

$$\theta_\mathrm{h} = 0, \quad \eta_\mathrm{h} = 1, \tag{13}$$

whereas for $A > 2$ two extra stationary homogeneous states exist in the model

$$\theta_{\mathrm{h}2,3} = \frac{A \mp \sqrt{A^2 - 4}}{2}, \quad \eta_{\mathrm{h}2,3} = \frac{A \pm \sqrt{A^2 - 4}}{2A}. \tag{14}$$

According to the general qualitative theory of ASs [11], pattern formation in systems of this kind is possible only when either $\epsilon \lesssim 1$ and/or $\alpha \lesssim 1$, so ϵ and α are in fact the natural small parameters of the model. Indeed, in the opposite case $\epsilon \gg 1$ and $\alpha \gg 1$ the dynamics of the inhibitor

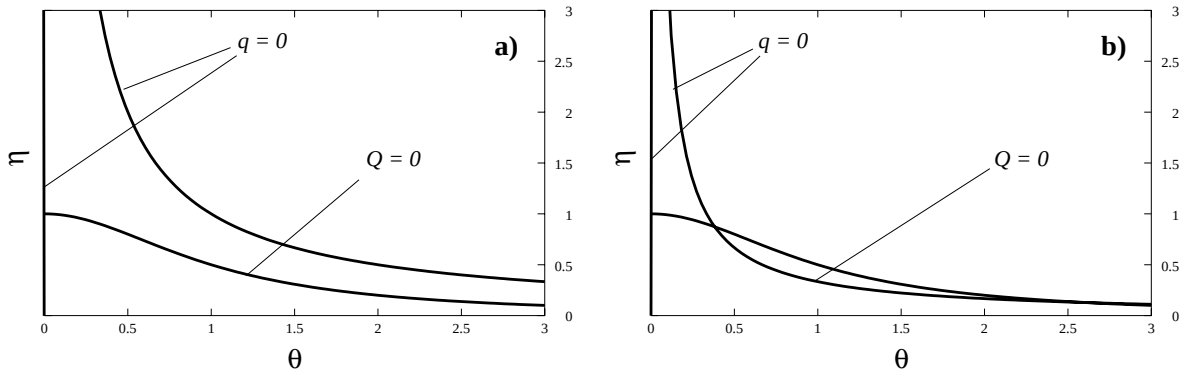

Fig. 1. The nullclines of equations (11) and (12) for (a) $A = 1$ and (b) $A = 3$.

becomes slaved to the activator, so we get a local relationship $\eta = \frac{1}{1+\theta^2}$ on the time and length scale of variation of the activator (see Eq. (12)). Substituting this back to equation (11) and rescaling length and time with ϵ and α, respectively, we obtain an effective equation for θ

$$\frac{\partial\theta}{\partial t} = \Delta\theta + \frac{A\theta^2}{1+\theta^2} - \theta. \tag{15}$$

This equation possesses a simple variational structure

$$\frac{\partial\theta}{\partial t} = -\frac{\delta\mathcal{F}}{\delta\theta}, \tag{16}$$

$$\mathcal{F} = \int \mathrm{d}^d x \left(\frac{(\nabla\theta)^2}{2} - A\theta + A\arctan\theta + \frac{\theta^2}{2} \right). \tag{17}$$

For $A < 2$ the functional $\mathcal{F}$ has a unique global minimum at $\theta = \theta_\mathrm{h} = 0$, so any initial condition will relax to the homogeneous state θ_h. For $A > 2$ there are two stable homogeneous states $\theta = \theta_\mathrm{h}$ and $\theta = \theta_{\mathrm{h}3}$ (see above), so it is possible to have waves of switching from one homogeneous state to the other [5]. It is easily checked that for $2 < A < 2.18$ the dominant homogeneous state is θ_h, while for $A > 2.18$ the dominant homogeneous state is $\theta_{\mathrm{h}3}$.

For $\epsilon \ll 1$ or $\alpha \ll 1$ the homogeneous state $\theta = \theta_{\mathrm{h}2}$, $\eta = \eta_{\mathrm{h}2}$ is always unstable. For $\epsilon \ll 1$ the homogeneous state $\theta = \theta_{\mathrm{h}3}$, $\eta = \eta_{\mathrm{h}3}$ is unstable with respect to the Turing instability if $A < 0.41\epsilon^{-1}$. For $\alpha \ll 1$ it is unstable with respect to the homogeneous oscillations (Hopf bifurcation) if $0.41\alpha^{-1/2} < A < \alpha^{-1/2}$, or it is an unstable node if $A < 0.41\alpha^{-1/2}$. On the other hand, the homogeneous state $\theta = \theta_\mathrm{h}$, $\eta = \eta_\mathrm{h}$ is stable for all values of the system's parameters. The latter is simple to understand: in order for the reaction to begin there has to be at least some amount of the activator substance put in at the start. Equivalently, the fact that the homogeneous state in equation (13) is stable for all values of the parameter A (for an arbitrary deviation from thermal equilibrium) is the consequence of the degeneracy (the presence of two separate branches, see Fig. 1) of the nullcline of equation (11). Thus, the self-organization associated with the Turing instability of the homogeneous state $\theta_\mathrm{h} = 0$ and $\eta_\mathrm{h} = 1$ is not realized in the Gray-Scott model. In such a stable homogeneous system any inhomogeneous pattern, including the ASs, can only be excited by a sufficiently strong external stimulus. In turn, self-organization will occur as a result of the instabilities of the large-amplitude patterns already present in the system.

To simulate equations (11) and (12) we used a simple explicit second-order scheme. In order to resolve the details of the shape of the spike, a sufficiently small spatial discretization step was needed. It was found that for the parameters used the step $\Delta x = 0.25\epsilon$ gave the solutions with the accuracy of a few per cent. The stiffness of the equations at small ϵ or α makes the simulations rather time consuming, so the simulations were done on a massively parallel supercomputer (SGI-Cray Origin 2000). A typical running time for the simulations shown in the paper is about 1 hour on 16 processors.

3 Pattern formations scenarios in two dimensions

Recently, we performed an extensive asymptotic analysis of the spike ASs in the Gray-Scott model with $\epsilon \ll 1$ and/or $\alpha \ll 1$ [35–37]. We identified different types of ASs and studied their stability [35–37, 41]. We found that at certain values of the parameters these ASs may undergo instabilities that should lead to the formation of more complex space-filling patterns. Here we present the results of the numerical simulations of the two-dimensional Gray-Scott model subject to localized stimuli that lead to the formation and destabilization of the ASs.

3.1 Granulation of the one-dimensional static spike autosoliton

According to the asymptotic theory, in two dimensions the static spike AS in the form of a stripe are unstable with respect to the corrugation instability with the length scale of order ϵ in the whole region of its existence [35, 41]. The growth of such a short-wave fluctuation should lead to the granulation of the stripe into small spots of size of order ϵ. To check that and the effect of curvature, we chose the

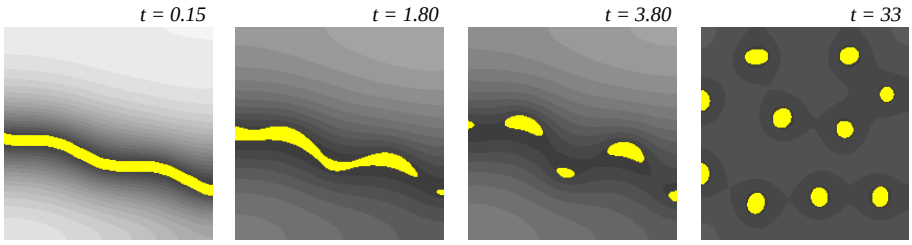

Fig. 2. Granulation of a stripe. Results of the numerical solution of equations (11) and (12) with $\epsilon = 0.05$, $\alpha = 0.5$, and $A = 2$. The system is 2.5×2.5. The shades of gray show the distribution of η. The spots show the regions where $\theta > 10$.

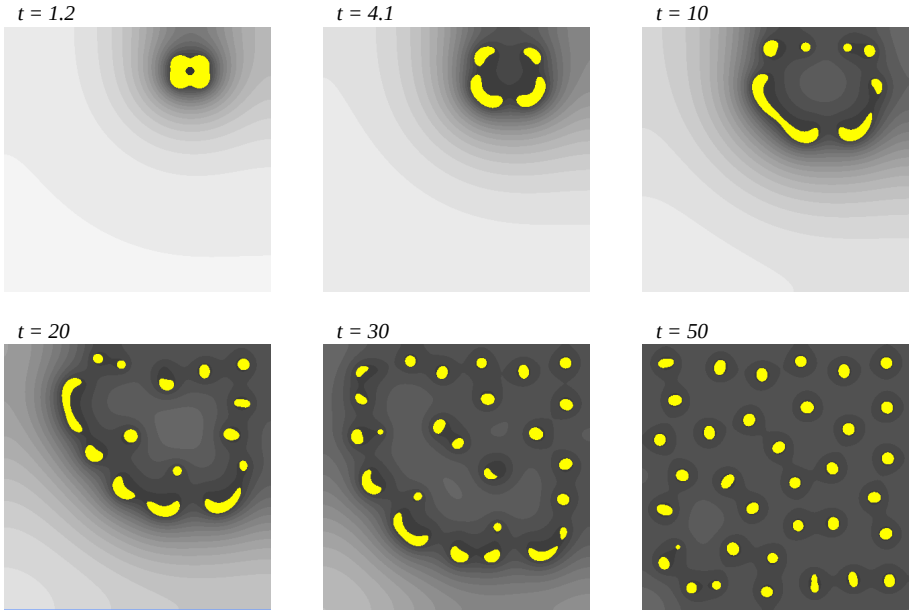

Fig. 3. Self-replication of spots in two dimensions. Results of the numerical solution of equations (11) and (12) with $\epsilon = 0.05$, $\alpha = 0.5$, and $A = 2$. The system is 5×5. The shades of gray show the distribution of η. The spots show the regions where $\theta > 10$.

initial condition in the form of a slightly wriggled stripe. Figure 2 shows this simulation with $\epsilon = 0.05$, $\alpha = 0.5$ and $A = 2$. One can see that the stripe indeed granulates to spots of size of order ϵ which then go away from each other until they become uniformly distributed across the system. The granulation initiates in the regions of high curvature of the stripe. Note that the self-replication of spots may occur during this process (see below).

3.2 Properties of the radially-symmetric static spike autosoliton

In [36], we asymptotically constructed the solutions in the form of the static radially-symmetric spike ASs (see also [40]). Our numerical simulations show that for $\epsilon \ll 1$ and $\alpha \gtrsim 1$ a localized stimulus applied to the system at $t = 0$ evolves into a stable static radially-symmetric spike AS in a relatively narrow range of values of A. Specifically, at $\epsilon = 0.05$ and sufficiently large values of α this happens at $0.38 < A < 0.65$. The amplitude of the static radially-symmetric spike AS is large in the entire range of A in which it exists. When α becomes sufficiently small, this region becomes even narrower since the AS becomes unstable with respect to the pulsations at sufficiently small A (*cf.* [35,41]). If this is the case, an initial stimulus may produce a localized pulsating state close to a radially-symmetric AS, which after several pulsations will collapse. When the value of α becomes smaller than some value α_c, the static radially-symmetric AS becomes unstable for all values of A and can no longer be excited. For $\epsilon = 0.05$ we found that $\alpha_c = 0.014 = 5.6\epsilon^2$.

3.3 Self-replication of the static radially-symmetric autosoliton

In [35, 41] we showed that when $\alpha \gtrsim 1$ and the value of A sufficiently large, the static radially-symmetric AS undergoes an instability with respect to a non radially-symmetric fluctuation. Our simulations confirm this prediction. The instability results in splitting and self-replication of the AS. For $\epsilon = 0.05$ and sufficiently large α the static radially-symmetric spike AS becomes unstable and self-replicates at $A \geq 0.7$. Such a process for $\epsilon = 0.05$, $\alpha = 0.5$, and $A = 2$ is shown in Figure 3. From this figure one can see that the initial condition in the form of

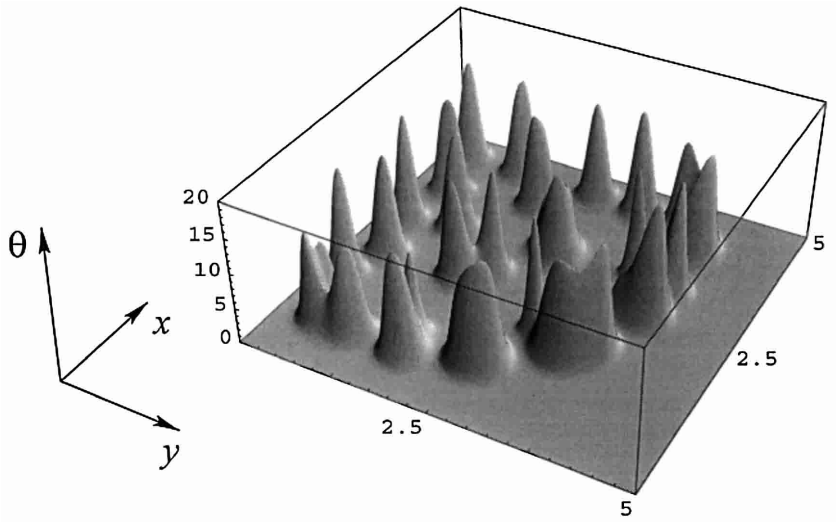

Fig. 4. Distribution of θ in the simulation of Figure 3 at $t = 30$.

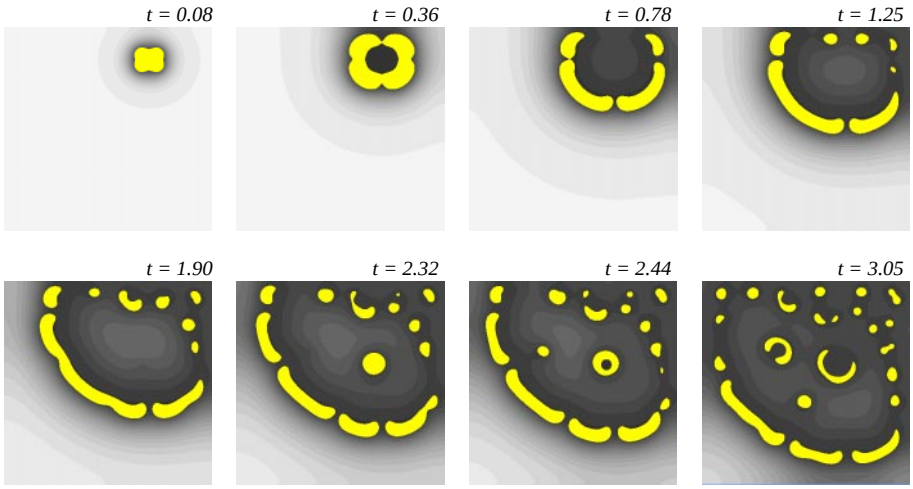

Fig. 5. Splitting as a result of the formation and the breakdown of a quasi one-dimensional wave. Results of the numerical solution of equations (11) and (12) with $\epsilon = 0.05$, $\alpha = 0.1$, and $A = 3$. The system is 5×5. The shades of gray show the distribution of η. The spots show the regions where $\theta > 10$.

a rectangle of size $\sim \epsilon$ splits into four (which is due to the rectangular shape of the initial condition and the fact that the value of A is well above the instability threshold), and then the newborn spots go on splitting. In the end the system gets filled with an irregular arrangement of spots, with the characteristic distance between the spots much less than 1. We would like to emphasize that the patterns observed in our simulations are essentially different from the domain patterns that form in systems of FitzHugh-Nagumo type, in which spot replication is also observed [20–24]. The distributions of the activator in our simulations consist of small spots instead of the domains with sharp interfaces. In the spots its distribution is close to that in the radially-symmetric static spike AS. This is illustrated in Figure 4 which shows the distribution of θ at $t = 30$ in Figure 3. When the value of α becomes small, the dynamics of splitting changes significantly. Figure 5 shows the evolution of the system with $\epsilon = 0.05$, $\alpha = 0.1$, $A = 3$, and a localized initial condition. In this case the pieces that form after splitting of an initial spot can go a greater distance apart and become more elongated than in Figure 3 (where $\alpha \sim 1$). The state that forms here is close to a torn-up quasi one-dimensional wave of width of order 1. This is natural to expect since, as we showed in [35,37], for these values of the parameters the traveling spike ASs may be realized in the system. In this case the formation of new spots occurs as a result of their pinching off the tips of the quasi one-dimensional wave pieces, that

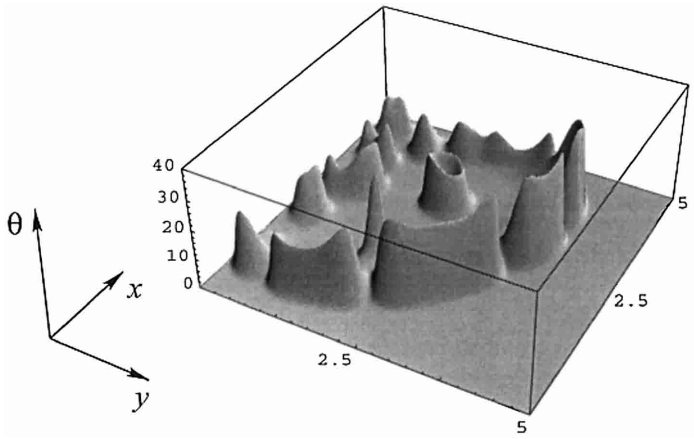

Fig. 6. Distribution of θ in the simulation of Figure 5 at $t = 2.44$.

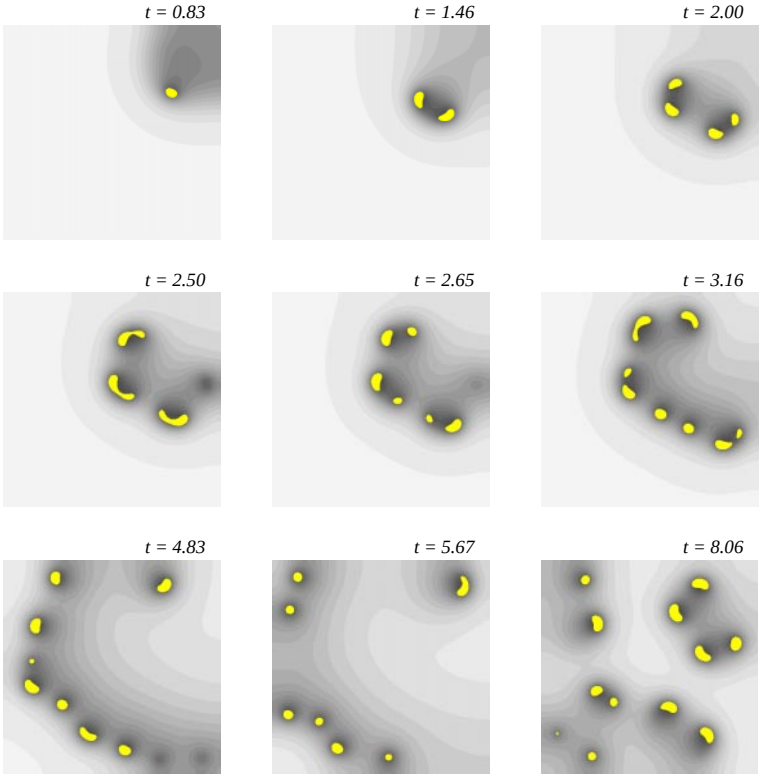

Fig. 7. Formation of spatio-temporal chaos. Results of the numerical solution of equations (11) and (12) with $\epsilon = 0.1$, $\alpha = 0.04$, and $A = 1$. The system is 10×10. The shades of gray show the distribution of η. The spots show the regions where $\theta > 5$.

is, they sort of drip from them. This process is illustrated in Figure 6 which shows the distribution of θ at $t = 2.44$ in Figure 5. The spots that drip from the wave pieces can further transform into quasi one-dimensional waves which in turn break up. As a result, the system becomes filled with a stable stationary pattern of spots, just as in the case of large α (see the last in Fig. 5).

3.4 Spatio-temporal chaos

For small enough values of α and A we were able to observe spatio-temporal chaos. Figure 7 shows the development of a chaotic pattern at $\epsilon = 0.1$, $\alpha = 0.04$, and $A = 1$. This pattern does not transform to a stationary pattern of spots even for very long simulation times ($t > 100$). The stochastization of the pattern is caused by random splitting of spots and the disappearance of some of the spots due to their annihilation upon collision with the bigger spots. According to our asymptotic theory [35,41], we would expect that these effects will be most pronounced when the static radially-symmetric AS is close to the instabilities with respect to the pulsations and the onset of the traveling motion (when $\alpha \sim \epsilon^2$), and is close to the instability with respect to splitting. Notice that such chaotic patterns are

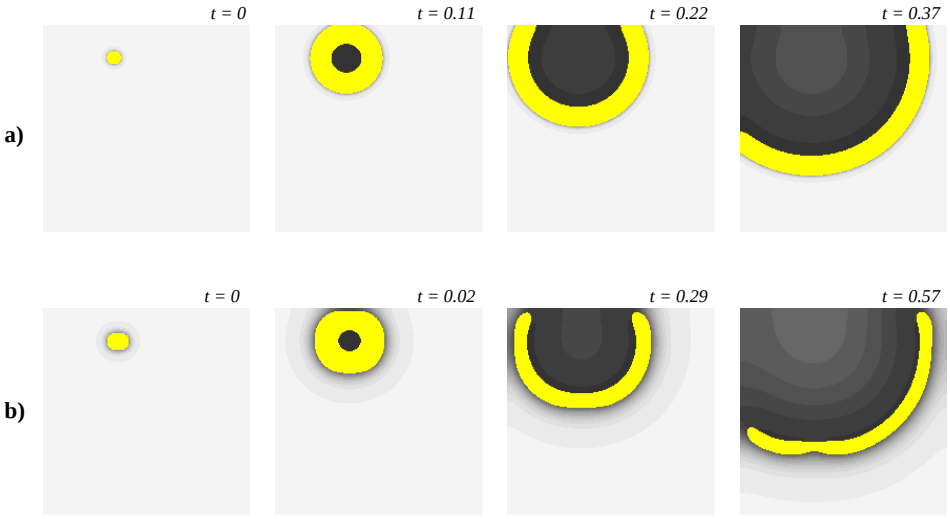

Fig. 8. Propagation of waves in the Gray-Scott model. Results of the numerical solution of equations (11) and (12) with (a) $\epsilon = 0.2$, $\alpha = 0.05$, and $A = 1.5$; (b) $\epsilon = 0.1$, $\alpha = 0.05$, $A = 1.5$. In (a) the system is 10×10; in (b) the system is 5×5. The shades of gray show the distribution of η. The spots show the regions where $\theta > 10$.

also observed in semiconductor structures [12], combustion systems [14], and chemical systems [15].

3.5 Radially diverging waves

For larger values of A and sufficiently small α an initially localized spot transforms into a circular stripe of growing radius (Fig. 8). When α is very small, this wave does not tear up and disappears at the system's boundary (Fig. 8a). When, on the other hand, α is not very small, the wave rebounds from the boundary and parts of it annihilate, so at some moment it tears up (Fig. 8b). The tips of this wave get repelled from the boundary, so the wave propagates across the system until it annihilates upon collision with the boundary at its opposite side.

4 Conclusion

Let us now summarize our observations of the pattern formation scenarios in the two-dimensional Gray-Scott model with $\epsilon \ll 1$ and/or $\alpha \ll 1$, subject to a localized stimulus. As was emphasized in Section 2, a special feature of the Gray-Scott model is the fact that in it the homogeneous state $\theta_{\rm h} = 0$, $\eta_{\rm h} = 1$ is stable for all values of the parameters. However, in such a stable homogeneous system it is possible to excite various steady inhomogeneous states, including self-sustained solitary inhomogeneous states, autosolitons (ASs), by applying a sufficiently strong external stimulus. The formation of these inhomogeneous states is due to self-production of substance X (the activator) controlled by substance Y (the inhibitor). The properties of the patterns are determined by only three parameters: ϵ, α, and A. The parameters $\epsilon = l/L$ and $\alpha = \tau_\theta/\tau_\eta$ are the ratios of the characteristic length and time scales of the activator and the inhibitor, respectively, and the control parameter A determines the degree of deviation of the system from equilibrium since it is proportional to the rate of supply of substance Y, which plays the role of "fuel" for the reaction in equation (1). We emphasize that for the same values of the system's parameters it is possible to excite *different* patterns which will be stable in certain ranges of the parameters ϵ, α, and A by choosing the form of the stimulus. At the stability margin the patterns spontaneously disappear or transform into the patterns of different kinds.

As follows from the general qualitative theory of the patterns in reaction-diffusion systems, the necessary condition for the existence of the persistent patterns of any kind is smallness of the parameters ϵ and/or α [9–11]. Depending on the values of ϵ and α, one can distinguish three different cases.

The first case corresponds to $\epsilon \ll 1$ and $\alpha \gtrsim 1$. As was expected from the general qualitative theory [9–11], for these values of ϵ and α one can excite only the static spike ASs whose amplitude $\theta_{\max} \gg 1$. In the two-dimensional Gray-Scott model with $\epsilon \ll 1$ and $\alpha \gtrsim 1$ one can excite the radially-symmetric static spike AS of size (in the dimensional units) of order l (Sect. 3). The range of values of A for which this AS exists is relatively narrow for $\epsilon \ll 1$. When the value of A is decreased, the static radially-symmetric spike AS, having large amplitude $\theta_{\max} \gg 1$, abruptly disappears. The range of A at which the radially-symmetric static spike AS exist becomes even narrower for small α when the AS becomes unstable with respect to the pulsations (Sect. 3). On the other hand, when the value of A is increased, the static radially-symmetric spike AS looses stability with respect to the radially non-symmetric fluctuations. As a result of the development of such fluctuations the AS splits into two, which then split in turn (self-replicate) until the system gets filled with a multispot pattern (Fig. 3). We would like to emphasize that for $\epsilon \ll 1$ a spot (a state close to the radially-symmetric AS) is the

dominant morphology, so that any localized initial state such as a stripe or a square first granulates into spots, and the evolution of the system is then governed by self-replication of these spots (Figs. 2, 3). Let us note that in FitzHugh-Nagumo type systems one sees complex patterns in the form of wriggling stripes, connected and disconnected labyrinthine patterns [20–24], which are also observed in chemical experiments [15]. These patterns do not form from a localized stimulus in the Gray-Scott model with $\epsilon \ll 1$. Note, however, that when $\epsilon \sim 1$, the Gray-Scott model starts behaving like a FitzHugh-Nagumo type system (see below), so for these values of ϵ such patterns can in fact be excited [26].

In the second case we have $\alpha \ll 1$ and $\epsilon \gtrsim 1$. In this case one can excite different kinds of self-sustained waves (autowaves) which in the cross-section have the form of the narrow spikes of size roughly l, the amplitude $\theta_{\max} \gg 1$ and the speed $c \gg l/\tau_\theta$ [35, 37]. Note that this type of waves is also realized in the Brusselator [44]. In two dimensions, besides the plane waves corresponding to the one-dimensional traveling spike ASs, one can excite the radially diverging waves (Fig. 8) and the steadily rotating spiral wave [45].

In the third case, when both ϵ and α are small, the behavior of the patterns in the Gray-Scott model is most diverse. The radially diverging traveling waves may undergo a transversal breakup leading to the formation of the stationary multispot patterns (Fig. 5). Also, when the values of α and A are small enough, one can excite the chaotic patterns (Fig. 7). The chaotic behavior of the latter is due to the random creation of new spots as a result of self-replication and annihilation of some of the spots as they collide with each other. This kind of spatio-temporal chaos is observed in chemical experiments [15] and is not unlike the one realized in FitzHugh-Nagumo type systems [22].

Let us comment on the relationship between the numerical simulations of the two-dimensional Gray-Scott model performed by Pearson in [26] and those of Section 3 performed by us. Pearson uses a different nondimensionalization of the Gray-Scott model, which has the following correspondence with our parameters [26]:

$$\epsilon^2 = \frac{D_v F}{D_u(F+k)}, \quad \alpha = \frac{F}{F+k}, \quad A = \frac{\sqrt{F}}{F+k}. \tag{18}$$

It is not difficult to see that for the simulations of Pearson $\epsilon \simeq 0.45$, $\alpha \simeq 0.4$, and $A \simeq 2$, so his choice of the parameters corresponds to $\epsilon \sim 1$ and $\alpha \sim \epsilon^2 \sim 1$. This is different from our simulations for which $\epsilon \ll 1$ and/or $\alpha \ll 1$. Note that the stationary patterns in the Gray-Scott model with $\epsilon \sim 1$ should actually resemble those forming in FitzHugh-Nagumo type systems [22]. Indeed, if one introduces the new variables $\tilde{\theta} = \frac{\theta}{A}$ and $\tilde{\eta} = \eta + \frac{\epsilon^2}{A}\theta$, after simple algebra one can write equations (11) and (12) as

$$\alpha \frac{\partial \tilde{\theta}}{\partial t} = \epsilon^2 \Delta \tilde{\theta} + A^2 \tilde{\theta}^2 \tilde{\eta} - \epsilon^2 A^2 \tilde{\theta}^3 - \tilde{\theta} \tag{19}$$

$$\frac{\partial \tilde{\eta}}{\partial t} = \Delta \tilde{\eta} + 1 - \tilde{\eta} - (1-\epsilon^2)\tilde{\theta} - (\alpha - \epsilon^2)\frac{\partial \tilde{\theta}}{\partial t}. \tag{20}$$

From equations (19) and (20) one can see that for $\epsilon \sim 1$ the nullcline of the equation for $\tilde{\theta}$ is actually cubic-like, and the coupling between $\tilde{\theta}$ and $\tilde{\eta}$ becomes linear, so the stationary patterns in this case should in fact look like those forming in FitzHugh-Nagumo type systems [22]. This is the reason why Pearson observed the stationary labyrinthine patterns, while in our simulations any stripe-like pattern always granulates into spots. Also, the collective oscillations of the space-filling patterns observed by Pearson are similar to the collective oscillations of the domain patterns in FitzHugh-Nagumo type systems [43]. Note that Pearson did not see the spiral waves observed by us in [45] because in his simulations $\alpha \sim \epsilon^2$ and the spirals break up as they form. We do not see any phase turbulence since in our simulations the system is far away from the Hopf bifurcation of the homogeneous state $\theta_{\mathrm{h}3}$, $\eta_{\mathrm{h}3}$. The rest of the patterns observed in [26] are similar to those observed by us.

We would like to acknowledge the computational support from the Center for Computational Science of Boston University.

References

1. G. Nicolis, I. Prigogine, *Self-Organization in Nonequilibrium Systems* (Wiley, New York, 1977).
2. V.A. Vasiliev, Y.M. Romanovskii, D.S. Chernavskii, V.G. Yakhno, *Autowave Processes in Kinetic Systems* (VEB Deutscher Verlag der Wissenschaften, Berlin, 1987).
3. *Oscillations and Traveling Waves in Chemical Systems*, edited by R.J. Field, M. Burger (Wiley, New York, 1985).
4. J.D. Murray, *Mathematical Biology* (Springer-Verlag, Berlin, 1989).
5. M.C. Cross, P.S. Hohenberg, Rev. Mod. Phys. **65**, 851 (1993).
6. A.S. Mikhailov, *Foundations of Synergetics* (Springer-Verlag, Berlin, 1990).
7. R. Kapral, K. Showalter, *Chemical Waves and Patterns* (Kluwer, Dordrecht, 1995).
8. B.S. Kerner, V.V. Osipov, in *Nonlinear Irreversible Processes*, edited by W. Ebeling, H. Ulbricht (Springer, Berlin, 1986).
9. B.S. Kerner, V.V. Osipov, Sov. Phys. Usp. **32**, 101 (1989).
10. B.S. Kerner, V.V. Osipov, Sov. Phys. Usp. **33**, 679 (1990).
11. B.S. Kerner, V.V. Osipov, *Autosolitons: a New Approach to Problem of Self-Organization and Turbulence* (Kluwer, Dordrecht, 1994).
12. *Nonlinear Dynamics and Pattern Formation in Semiconductors and Devices*, edited by F.J. Niedernostheide (Springer, Berlin, 1994).
13. M. Bode, H.G. Purwins, Physica D **86**, 53 (1995).
14. M. Gorman, M. el Hamdi, K.A. Robbins, Combust. Sci. Tech. **98**, 37 (1994); *ibid.* 71; *ibid.* 79.
15. K.J. Lee, W.D. McCormick, Q. Ouyong, H.L. Swinney, Science **261**, 192 (1993); K.J. Lee, W.D. McCormick, J.E. Pearson, H.L. Swinney, Nature **369**, 215 (1994); K.J. Lee, H.L. Swinney, Phys. Rev. E **51**, 1899 (1995).
16. B.S. Kerner, V.V. Osipov, Sov. Phys. JETP **47**, 874 (1978); Biophysics (USSR) **27**, 138 (1982); Sov. Phys. JETP Lett. **41**, 473 (1985).

17. B.S. Kerner, V.V. Osipov, Sov. Phys. Semicond. **13**, 424 (1979); B.S. Kerner, V.V. Osipov, Sov. Phys. Solid State **21**, 1348 (1979).
18. B.S. Kerner, V.V. Osipov, Sov. Phys. JETP **52**, 1122 (1980); Sov. Microelectronics **10**, 407 (1981).
19. S. Koga, Y. Kuramoto, Prog. Theor. Phys. **63**, 106 (1980).
20. D.M. Petrich, R.E. Goldstein, Phys. Rev. Lett. **72**, 1120 (1994); R.E. Goldstein, D.J. Muraki, D.M. Petrich, Phys. Rev. E, **53**, 3933 (1996).
21. C.B. Muratov, V.V. Osipov, Phys. Rev. E **53**, 3101 (1996).
22. C.B. Muratov, V.V. Osipov, Phys. Rev. E **54**, 4860 (1996).
23. A. Hagberg, E. Meron, Phys. Rev. Lett. **72**, 2492 (1994); A. Hagberg, E. Meron, Chaos **4**, 477 (1994); C. Elphick, A. Hagberg, E. Meron, Phys. Rev. E **51**, 3052 (1995).
24. C.B. Muratov, Ph.D. Thesis, Boston University, 1997.
25. B.S. Kerner, V.V. Osipov, Sov. Phys. JETP **62**, 337 (1985).
26. J.E. Pearson, Science **261**, 189 (1993).
27. P.J. Ortoleva, J. Ross, J. Chem. Phys. **63**, 3398 (1975); P. Ortoleva, R. Sultan, J. Chem. Phys. **148**, 47 (1990); R.G. Casten, H. Cohen, A. Lagerstrom, Quart. Appl. Math. **32**, 365 (1975).
28. B.S. Kerner, V.V. Osipov, Sov. Phys. JETP **56**, 1275 (1982); V.V. Gafiichuk, B.S. Kerner, I.M. Lazurchak, V.V. Osipov, Mikroelektronika **15**, 180 (1986); V.V. Osipov, V.V. Gafiichuk, B.S. Kerner, I.M. Lazurchak, Mikroelektronika **16**, 23 (1987); V.V. Gafiichuk, V.E. Gashpar, B.S. Kerner, V.V. Osipov, Sov. Phys. Semicond. **22**, 1298 (1988).
29. B.S. Kerner, V.V. Osipov, Mikroelektronika **12**, 512 (1983); J.D. Dockery, J.P. Keener, SIAM J. Appl. Math. **49**, 539 (1989).
30. E.M. Kuznetsova, V.V. Osipov, Phys. Rev. E **51**, 148 (1995).
31. K. Krischer, A. Mikhailov, Phys. Rev. Lett. **73**, 3165 (1994).
32. P. Schutz, M. Bode, V.V. Gafiichuk, Phys. Rev. E **52**, 4465 (1995).
33. V.V. Osipov, Physica D **93**, 143 (1996).
34. P. Gray, S. Scott, Chem. Eng. Sci. **38**, 29 (1983).
35. C.B. Muratov, V.V. Osipov, CAMS Rep. 9900-10, NJIT, Newark, NJ 07102 (available at LANL archive: `patt-sol/9804001`).
36. C.B. Muratov, V.V. Osipov, J. Phys. A **33**, 8893 (2000).
37. C.B. Muratov, V.V. Osipov, Physica D **155**, 112 (2001).
38. A. Doelman, T.J. Kaper, P. Zegeling, Nonlinearity **10**, 523 (1997); A. Doelman, R.A. Gardner, T.J. Kaper, Physica D **122**, 1 (1998).
39. J.K. Hale, L.A. Peletier, W.C. Troy, SIAM J. Appl. Math. **61**, 102 (2000).
40. J.C. Wei, Physica D **148**, 20 (2001).
41. C.B. Muratov, V.V. Osipov, SIAM J. Appl. Math. (submitted).
42. C.B. Muratov, Phys. Rev. E **54**, 3369 (1996).
43. C.B. Muratov, Phys. Rev. E **55**, 1463 (1997).
44. V.V. Osipov, C.B. Muratov, Phys. Rev. Lett. **75**, 388 (1995).
45. C.B. Muratov, V.V. Osipov, Phys. Rev. E **60**, 242 (1999).